

The Structures of Sulfate, Sulfite and Disulfite Ions in Aqueous Solution Determined by X-Ray Diffraction

TOSHIO YAMAGUCHI and OLIVER LINDQVIST

Department of Inorganic Chemistry, Chalmers University of Technology and the University of Göteborg, S-412 96 Göteborg, Sweden

X-Ray scattering measurements were carried out at 25 °C for concentrated aqueous solutions of ammonium sulfate (pH=4.8), ammonium sulfite (pH=8.3) and ammonium disulfite (pH=5.5 and 5.1). Intensity data were analyzed in terms of the radial distribution functions and reduced intensities. The sulfate ion has a tetrahedral structure with an S–O distance of 1.481(3) Å, while the sulfite ion has a pyramidal C_{3v} structure. The S–O distance within SO_3^{2-} is 1.529(4) Å; the lone-pair of electrons of S(IV) is stereochemically active in solution. The $S_2O_5^{2-}$ ion has an S–S bridge with a bond length of 2.221(11) Å. The S–O distances of the thionite and thionate groups could not be distinguished, but the average S–O distance is 1.498(2) Å. Plausible hydration models of the ions are discussed.

The equilibrium species resulting when dissolving sulfur dioxide in water have been extensively studied by spectroscopic techniques. The interest in this system arises not only from a theoretical point of view but also from the needs in practical fields, i.e. research on SO_2 -induced atmospheric corrosion¹ and catalytic oxidation of SO_2 in polluted air.²

The sulfite ion, SO_3^{2-} , the hydrogen sulfite ion, HSO_3^- , and the disulfite ion, $S_2O_5^{2-}$, occur in equilibrium in aqueous solution, the equilibrium constants being reported by Bourne *et al.*³ Raman spectra of an Na_2SO_3 aqueous solution have indicated that the sulfite ion has a pyramidal C_{3v} structure.⁴ However, much controversy has persisted for more than 100 years regarding the structures of the HSO_3^- and $S_2O_5^{2-}$ ions. The structure of the hydrogen sulfite ion was first proposed by Simon *et al.*⁵ to have pyramidal C_{3v} structure containing an H–S bond. Their result was based on the Raman spectra of cesium hydrogen sulfite. Recently, this

structure was confirmed both by isotopic Raman spectroscopic measurements of $CsHSO_3$,⁶ where all six fundamentals of the bisulfite ion were observed and assigned, and by X-ray and neutron crystal structure determinations of $CsHSO_3$.⁷ The existence of both $HOSO_2^-$ and HSO_3^- ions in solution has been suggested⁹ but the equilibrium distribution is not known. Concerning the disulfite ion, Simon *et al.*⁸ originally proposed a symmetrical $O_2SOSO_2^{2-}$ structure from Raman spectra of potassium salts in the solid state and in solution. However, he later changed his assignments of the bands, accepting the S–S bridge giving an $O_3SSO_2^{2-}$ structure with C_s symmetry,⁵ later confirmed in other investigations.^{4,6,9} X-Ray structural analyses of $K_2S_2O_5$ ¹⁰ and $(NH_4)_2S_2O_5$ ¹¹ confirmed the C_s symmetry containing the S–S bond in the solid state.

Tautomeric structures of both hydrogen sulfite and disulfite ions may occur in solution since the assignment of Raman bands of such solutions is incomplete.⁶ In the present investigation, the X-ray diffraction method was applied to determine the structures of sulfite and disulfite ions in aqueous solution. The ammonium ion was chosen as cation, since it fits well into the bulk water structure. Thus, the structure of anion hydration will not be seriously disturbed by that of cation hydration. Besides, ammonium sulfite and ammonium disulfite are more soluble in water than other salts,¹² which makes the data analyses more accurate. In order to discuss the S–O bond distances and the hydration of the SO_3^{2-} and $S_2O_5^{2-}$ ions in solution, it was considered profitable to make comparisons with an SO_4^{2-} solution. Recently, Caminiti *et al.*¹³ investigated a concentrated ammonium sulfate solution with X-ray diffraction techniques. In their

Table 1. Compositions of the solutions (mol dm⁻³). *V* is the stoichiometric volume (Å³) per sulfur atom, μ the linear absorption coefficient (cm⁻¹) and *d* the density (g cm⁻³).

	(NH ₄) ₂ SO ₄	(NH ₄) ₂ SO ₃	(NH ₄) ₂ S ₂ O ₅	(NH ₄) ₂ S ₂ O ₅
S	3.900	3.711	8.314	10.92
O	55.59	52.94	50.60	51.31
N	7.800	7.542	11.20	11.35
H	111.2	113.8	101.5	92.99
pH	4.8	8.3	5.3	5.1
<i>V</i>	425.8	440.4	199.7	152.1
μ	2.50	2.40	3.79	4.60
<i>d</i>	1.236	1.191	1.335	1.424

analysis, however, the S–O interaction within the SO₄²⁻ ion was subtracted as a known parameter. Therefore, but also to study the hydration of the sulfate ion, we decided to include a reinvestigation of an ammonium sulfate solution in the present work. Raman spectral measurements have also been carried out to identify the main species in the solutions used in the X-ray experiments.

EXPERIMENTAL

Preparation and analysis of sample solutions

Since the equilibrium, $2\text{HSO}_3^- \rightleftharpoons \text{S}_2\text{O}_5^{2-} + \text{H}_2\text{O}$, inclines to the right-hand side with increasing concentration,³ it is not possible to prepare an HSO₃⁻ solution suitable for the X-ray analysis.

Solutions of ammonium sulfite (pH=8.3) and ammonium disulfite (pH=5.3 and 5.1) were prepared under nitrogen atmosphere by dissolving gaseous SO₂ in a cold solution (ca. 0 °C), which had previously been saturated with ammonia, until the required pH was obtained. pH determinations were made by means of a Radiometer Model 29 pH-meter, calibrated with a buffer solution (Merck, pH=4.0).

A saturated solution of ammonium sulfate was prepared by dissolving ammonium sulfate (Merck, pro analysi), without further purification, into distilled water.

The concentrations of the sulfite and the disulfite solutions were determined by oxidation to sulfate with hydrogen peroxide. The sulfate was analyzed gravimetrically as BaSO₄. The content of ammonium was determined by the Kjeldahl method.¹⁴ The solution densities were measured with pycnometers. The compositions of the sample solutions are given in Table 1.

X-Ray measurements

X-Ray scattering measurements were carried out at 25 °C by a θ – θ diffractometer of the same type as described elsewhere¹⁵ with a bent LiF monochromator in the diffracted beam. MoK α radiation ($\lambda = 0.7107$ Å) was used, a 2 kW fine focus X-ray tube being employed. The sample solution, contained in a flat teflon tray (inner diameter 40 mm and depth 10 mm) was enclosed in an airtight shield with a cylindrical Be window for X-rays. During the measurements of sulfite and disulfite solutions, the inside of the container was filled with nitrogen gas to prevent oxidation. The scattered intensities were collected by a step scanning mode at discrete points over the range of scattering angle (2θ) from 2 to 130°, corresponding to the range $0.3 \leq s \leq 16.0$ Å⁻¹ ($s = 4\pi \sin \theta / \lambda$). The intervals of 0.1 and 0.25° were used, respectively, for the range of $1 \leq \theta \leq 20$ and $20 \leq \theta \leq 65$ °. Measurements were repeated until total counts at each data point amounted to 80000 ($1 \leq \theta \leq 10$ °) and 120000 ($10 \leq \theta \leq 65$ °). Pairs of divergent and scattering slits of 1/12–1/2°, 1/6–1/2° and 1–1° were used for the ranges $1^\circ \leq \theta \leq 8^\circ$, $3^\circ \leq \theta \leq 12^\circ$ and $8^\circ \leq \theta \leq 65^\circ$, respectively.

Data analysis

Experimental intensities, corrected for background,¹⁶ absorption,¹⁷ double scattering,¹⁸ polarization¹⁹ and Compton radiation,²⁰ were scaled to absolute units by comparison of measured intensities with the total independent theoretical scattering in a high angle region ($s \geq 13.5$ Å⁻¹). The scaling factor thus obtained agreed within 2% with that calculated by the Krogh-Moe²¹ and the Norman²² methods. The scattering factors for neutral atoms were taken from the International Tables for X-Ray Crystallography,²³ except H₂O for which molecular form factors proposed by Hajdu²⁴ were used. The values for incoherent scattering factors were taken

from those given by Cromer and Mann²⁵ for N, by Cromer²⁶ for O and S, by Compton and Allison²⁷ for H, and by Hajdu²⁴ for H₂O. The incoherent scattering factors were corrected for the Breit-Dirac effect.^{28,29} The values for anomalous dispersion were taken from the International Tables for X-Ray Crystallography.²³ The reduced intensities, $i(s)$, were derived from eqn. (1), where $I(s)_{\text{obs}}$ is the

$$i(s)_{\text{obs}} = I(s)_{\text{obs}} - \sum n_i \{ (f_i(s) + \Delta f_i')^2 + (\Delta f_i'')^2 \} \quad (1)$$

scaled measured intensities, n_i the number of atom "i" in a stoichiometric volume V containing one S atom, f_i , $\Delta f_i'$ and $\Delta f_i''$ the scattering factor, the real and imaginary parts of anomalous dispersion of atom "i", respectively. The electronic radial distribution function, $D(r)$, was then obtained by Fourier inversion (2). Here ρ_0 represents the average

$$D(r) = 4\pi r^2 \rho_0 + \frac{2r}{\pi} \sum_0^{s_{\text{max}}} s \cdot i(s) M(s) \sin(rs) \Delta s \quad (2)$$

scattering density $\{ [\sum n_i f_i(0) + \Delta f_i']^2 + (\sum n_i \Delta f_i'')^2 \} / V$, the modification function $M(s)$ is $\{ (f_s(0) + \Delta f_s')^2 + (\Delta f_s'')^2 \} / \{ (f_s(s) + \Delta f_s')^2 + (\Delta f_s'')^2 \} \exp(-0.01s^2)$ and s_{max} , the maximum value of s available in each experiment. Spurious ripples observed in a hard-core region of the $D(r)$ function were removed in the usual manner.¹⁹

Theoretical reduced intensities based on models were calculated by eqn. (3), where r_{ij} , b_{ij} and n_{ij}

$$\frac{i(s)_{\text{calc}}}{\sin(rs)} = \frac{\sum \sum n_{ij} \{ (f_i(s) + \Delta f_i')(f_j(s) + \Delta f_j') + (\Delta f_i'')(\Delta f_j'') \}}{\exp(-b_{ij}s^2)} \quad (3)$$

denote the distance, the temperature factor and the frequency factor of a pair of atoms, "i-j". The corresponding peak shapes were obtained by Fourier transformation [eqn. (2)]. These calculations were carried out by means of the KURVLR program.³⁰

For a quantitative analysis, the least-squares method was applied to the reduced intensities, the function $\sum_{s_{\text{min}}}^{s_{\text{max}}} w(s) \{ i(s)_{\text{obs}} - i(s)_{\text{calc}} \}^2$ being minimized by means of the NLPLSQ program.³¹ The weighting function $w(s)$ was proportional to $I_{\text{obs}}^{-2} \cos \theta$. Lower and upper values s_{min} and s_{max} were set for adequate model fitting.

Raman measurements

Raman spectra were recorded with a Cary 82 laser Raman spectrophotometer using the 4880 Å excited line of an argon laser. The solutions were contained in glass tubes of 1 mm diameter.

RESULTS AND DISCUSSION

1. Solution of ammonium sulfate (pH = 4.8)

Fig. 1A shows the radial distribution curve, $D(r) - 4\pi r^2 \rho_0$, for the (NH₄)₂SO₄ solution. The general features of the distribution curve are similar to those obtained by Caminiti *et al.*,¹³ except for the S-O peak at 1.5 Å subtracted from their data. The O-O interaction within the sulfate ion contributes to a shoulder around 2.40 Å. The 2.90 Å peak is typical for aqueous solution, attributed to the first neighbor H₂O-H₂O (or H₂O-NH₄⁺) interaction in the bulk structure.³² The peak around 3.80 Å can be ascribed to the interaction between the S atom in the sulfate ion and hydration water molecules, as Caminiti *et al.* suggested.¹³ The shoulder at 4.80 Å and the broad peak observable at 6.0-7.2 Å reflect long-range interactions which are difficult to interpret in detail.

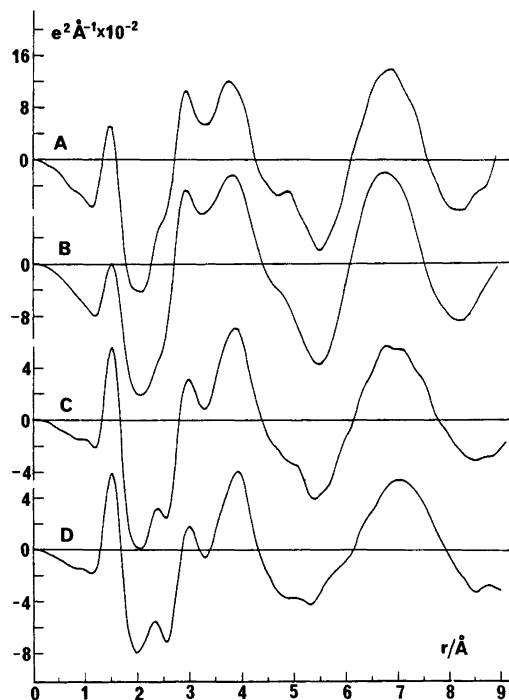


Fig. 1. Experimental radial distribution curves, $D(r) - 4\pi r^2 \rho_0$, of the solutions investigated. (A) (NH₄)₂SO₄ (pH = 4.8), (B) (NH₄)₂SO₃ (pH = 8.3), (C) (NH₄)₂S₂O₅ (pH = 5.3), (D) (NH₄)₂S₂O₅ (pH = 5.1).

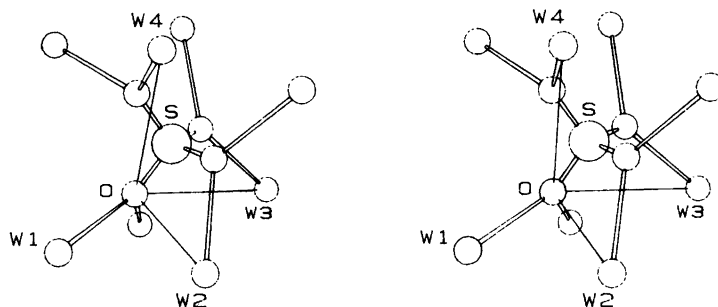


Fig. 2. A symmetric hydration model of the sulfate ion (stereoview).

From the dissociation constant³³ of the HSO_4^- ion and the measured pH value of 4.8 in the sample solution, it can be calculated that the SO_4^{2-} ion should dominate completely. Thus, the model adopted for the analysis had the following characteristics.

- (a) A tetrahedral sulfate ion described by parameters $r_{\text{S-O}}$, $b_{\text{S-O}}$ and $b_{\text{O-O}}$.
 (b) Hydration of the SO_4^{2-} with S-H₂O inter-

actions described by three parameters $r_{\text{S-W}}$, $b_{\text{S-W}}$ and $n_{\text{S-W}}$. Interactions between sulfate oxygen atoms and hydration water molecules were also taken into account.

(c) The bulk structure was treated as that of pure water and calculated by using Narten's original data (cf. Ref. 32).

In a first step of refinement, parameter $n_{\text{S-W}}$ was refined independently to estimate the number of

Table 2. Results of least-squares refinements A, B and C (see text) for the $(\text{NH}_4)_2\text{SO}_4$ solution obtained in the range $2.0 \leq s \leq 15.0 \text{ \AA}^{-1}$. Standard deviations are given in parentheses.

		A	B	C
S-O	<i>r</i>	1.464(5)	1.481(2)	1.480 ^c
	<i>b</i>	0.0008(4)	0.0011(2)	0.0005(4)
	<i>n</i>	4	4	4
O-O	<i>r</i>	2.391 ^a	2.418 ^a	2.417
	<i>b</i>	0.059(6)	0.0036(7)	0.0016
	<i>n</i>	6	6	6
S-W	<i>r</i>	3.45(4)	3.70(1)	3.64 ^c
	<i>b</i>	0.06(2)	0.020(1)	0.064(7)
	<i>n</i>	8	8	8
O-W(1)	<i>r</i>	2.48 ^b	2.86(1)	2.66 ^c
	<i>b</i>	0.023(4)	0.004(1)	0.039(7)
	<i>n</i>	8	8	8
O-W(2)	<i>r</i>	3.28 ^b	3.17(2)	3.20 ^c
	<i>b</i>	0.08(2)	0.009(1)	0.008(6)
	<i>n</i>	4	4	4
O-W(3)	<i>r</i>	3.70 ^b	4.05(3)	4.06 ^c
	<i>b</i>	0.045(12)	0.009(2)	0.086(16)
	<i>n</i>	8	8	8
O-W(4)	<i>r</i>	4.43 ^b	4.67(5)	4.53 ^c
	<i>b</i>	0.045(20)	0.034(3)	0.42(9)
	<i>n</i>	8	8	8
R-factor ^d		0.340	0.114	0.317

^a Fixed to the value ($=\sqrt{8/3} \times r_{\text{S-O}}$). ^b Estimated from the geometry shown in Fig. 2. ^c Average distances found in the crystal structure.³⁴ ^d $R = \{\sum s^2 \Delta i(s)^2 / \sum s^2 i(s)_{\text{obs}}^2\}^{1/2}$ with $\Delta i(s) = i(s)_{\text{obs}} - i(s)_{\text{calc}}$.

water molecules bonded to the sulfate ion. In agreement with the result obtained by Caminiti *et al.*,¹³ $n_{S-W} = \sim 8$ was obtained. The construction of a complete hydration model of the SO₄²⁻ ion seemed difficult since the distribution curve does not give any clear indication about the hydration geometry. Crystal structures are sometimes comparable with the geometry in solution. Kjällman and Olovsson³⁴ have determined the crystal structure of H₂SO₄·4H₂O, in which two water molecules are hydrogen bonded to each sulfate oxygen atom. Based on this structure, we built up a symmetric hydration model with W–O–W angles of 120° and minimum W–W repulsion as shown in Fig. 2. Least-squares calculations were carried out in various ways as summarized in Table 2.

In refinement A, the distances of the S–O and the S–W interactions were refined, while other distances were fixed to the values based on the geometry of the symmetric model. The temperature factors of all interactions were allowed to vary

independently. In refinement B, only the assumption of the tetrahedral SO₄²⁻ structure hydrated by eight water molecules was retained, while all the other parameters of the model were allowed to vary. As a comparison, refinement C was also carried out using distances reported in the actual crystal³⁴ with all the temperature factors as adjustable parameters.

The S–O distance obtained in refinement B was in good agreement with the average value in the solid state, while that in refinement A is somewhat shorter but still falls in the range of S–O distances reported for sulfate salts.³⁵ Also other interaction distances obtained in refinement B were consistent with the corresponding distances in the crystal, except the O–W(1) distance. The refinement was carried out, however, based on a simple assumption concerning the bulk structure, which may affect the O–W(1) interaction.

The distances of the S–W and O–W(3) interactions obtained in refinement A are significantly

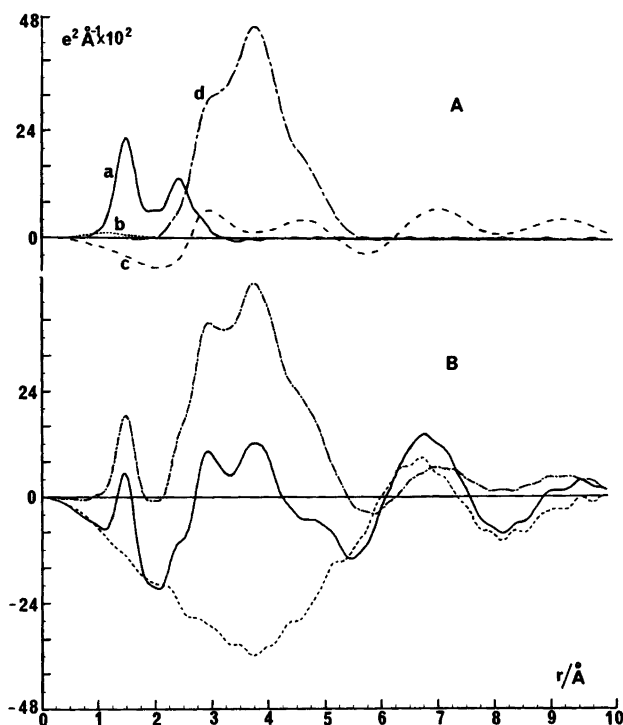


Fig. 3. (A) Peak shapes calculated for (a) the SO₄²⁻ ion, (b) the NH₄⁺ ion, (c) the bulk structure and (d) the hydration structure of the SO₄²⁻ ion (S–W, O–W(1), O–W(2), O–W(3) and O–W(4)). (B) Experimental (—) and theoretical (---) radial distribution curves with their difference (· · ·) for the (NH₄)₂SO₄ solution.

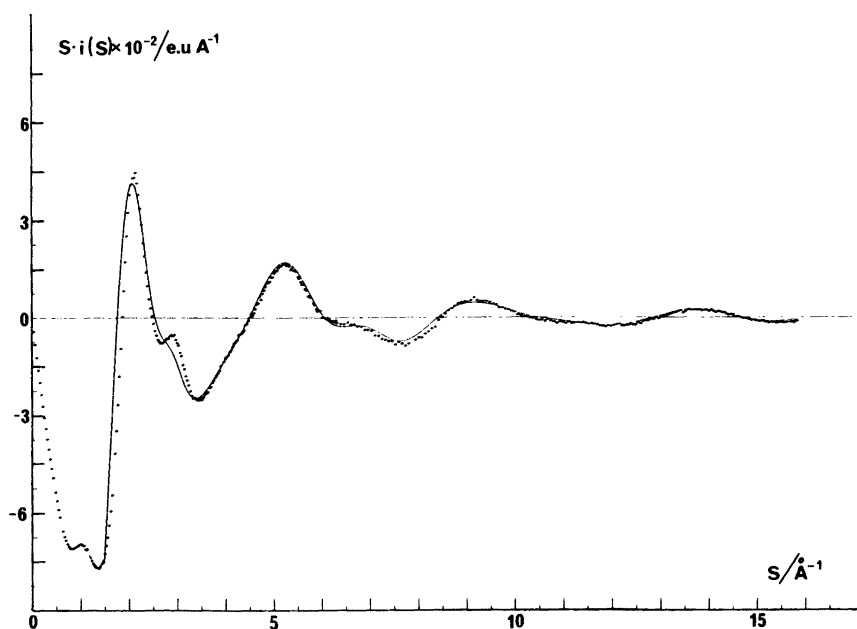


Fig. 4. Observed (dots) and calculated (solid line) $s \cdot i(s)$ values for the $(\text{NH}_4)_2\text{SO}_4$ solution.

shorter than those in refinements B and C. It is therefore reasonable to assume that the water molecules are not as rigidly hydrogen bonded to the SO_4^{2-} ion as suggested in the symmetric model in Fig. 2. The basic results of refinement B as a time average, *i.e.* a hydration sphere containing eight water molecules at ~ 3.7 Å from the center of the SO_4^{2-} ion, having hydrogen bond distances [O–W(1)] of ~ 2.85 Å, are thus strongly supported by the experimental data. The distances O–W(2), O–W(3) and O–W(4) probably include long-range interactions.

Fig. 3 A shows the individual theoretical contributions to the radial distribution curve from (1) the SO_4^{2-} ion, (2) the hydration of the SO_4^{2-} ion and (3) the bulk structure according to model B. Fig. 3 B shows the experimental distribution curve and theoretical peak shape with their difference.

Fig. 4 shows observed $s \cdot i(s)$ values compared to the values calculated from model B.

2. Solution of ammonium sulfite (pH = 8.3)

Fig. 1 B represents the radial distribution curve of the ammonium sulfite solution. The 1.5 Å peak can be ascribed to the S–O bonds within the

sulfite ion, being in agreement with the results of crystal structure determination.^{36–41} The area under the peak corresponds to approximately three S–O bonds within the sulfite ion. The shoulder around 2.4 Å may be due to the O–O bonds within the SO_3^{2-} ion. The peak centered at 2.9 Å can be attributed to the bulk structure.³² The interaction between sulfite oxygen atoms and hydration water molecules may also contribute partly to this peak. The peak observed at 3.8 Å may indicate the hydration of the SO_3^{2-} ion as found in the sulfate solution.

The structure of the ammonium sulfite solution was analyzed by means of least-squares calculations in the following way.

(a) The structure of the sulfite ion was first described by distances ($r_{\text{S-O}}$ and $r_{\text{O-O}}$) and temperature factors ($b_{\text{S-O}}$ and $b_{\text{O-O}}$) of the S–O and O–O bonds since the O–S–O bond angle cannot be postulated in the sulfite ion. In some preliminary refinements, however, the O–O distance converged to unreasonable values, probably because of its small contribution to the intensity data. Therefore, the O–O distance was fixed to the value estimated from the radial distribution curve, also being in accordance with the results of crystal structure determinations.^{36–41} This restriction is relevant, since the O–O distance in the sulfite ion does not

Table 3. Results of least-squares refinements A, B and C (see text) for the (NH₄)₂SO₃ solution obtained in the range 2.0 ≤ s ≤ 15.0 Å⁻¹. Standard deviations are given in parentheses.

		A	B	C
S—O	r	1.529(4)	1.524 ^b	1.517(8)
	b	0.0021(3)	0.0017(4)	0.0033(7)
	n	3	3	3
O—O	r	2.42 ^a	2.414 ^b	2.85(11)
	b	0.005(2)	0.002	0.014(7)
	n	3	3	3
S—W	r	3.79(2)	3.80 ^b	3.73(4)
	b	0.022(1)	0.064	0.050(3)
	n	8	9	12
O—W(1)	r	2.81(3)	2.82 ^b	2.85(3)
	b	0.020(3)	0.005(1)	0.005(2)
	n	6	9	9
O—W(2)	r	3.23(4)	3.60 ^b	3.01(23)
	b	0.024(3)	0.015(8)	0.11(3)
	n	7	5	9
O—W(3)	r	4.22(7)	4.21 ^b	4.30(9)
	b	0.013(4)	0.10(5)	0.015(4)
	n	6	4	9
O—W(4)	r	4.59(7)	4.75 ^b	4.71(12)
	b	0.009(3)	0.011(5)	0.011(6)
	n	6	5	9
R-factor		0.119	0.311	0.253

^a The value estimated from the distribution curve, in accordance with the crystal structures.³⁶⁻⁴¹ ^b Average distances found in the crystal structures.

change significantly with the S—O distance as discussed by Kierkegaard *et al.*⁴²

(b) The interactions between the sulfite ion and hydration water molecules are described by the S—W (*r*_{S-W}, *b*_{S-W} and *n*_{S-W}) and O—W (*r*_{O-W}, *b*_{O-W} and *n*_{O-W}) parameters obtained from different models.

(c) The contribution from the bulk structure was calculated in a manner similar to that described in the previous section.

Table 3 summarizes the results of the least-squares refinements. Refinement A is based on a hydration model (Fig. 5 A), in which two water molecules are bonded to each sulfite oxygen atom as found for the sulfate ion. In addition, there are two more water molecules located toward the lone-pair of electrons of S(IV). Model B (Fig. 5 B) was constructed from the crystal structure of (NH₄)₂SO₃·H₂O.^{36,37} A third refinement was based on the MgSO₃·6H₂O³⁸ structure (Fig. 5 C). In this structure each sulfite oxygen is hydrogen bonded to three water molecules at distances 2.66–2.72 Å and three more water molecules lie on the lone-pair

side of the S atom.

The refinement results of hydration models A and B are rather comparable, except for the O—W(2) distance which may be affected by the bulk structure. Hydration model C was refined in two ways, *i.e.* (1) restricted to the geometry found in the MgSO₃·6H₂O crystal (R=0.63) and (2) unrestricted as shown in Table 3 C (R=0.25). From the results given in Table 3, it can be concluded that the sulfite ion is surrounded by 8–9 water molecules at an S—W distance of ~3.8 Å, according to model A. The O—W(1) hydrogen bond distance is of the same order of magnitude as in the sulfate solution, *i.e.* ~2.8 Å. The O—W(2), O—W(3) and O—W(4) interactions are influenced by the bulk structure, and may be regarded as model fitting parameters.

The S—O bond length in the sulfite ion was found to be 1.529(4) Å, which agrees well with those found in hydrogen bonded sulfite ions in crystals, *e.g.* 1.536 Å (NiSO₃·6H₂O⁴¹), 1.517 Å³⁷ and 1.529 Å³⁶ ((NH₄)₂SO₃·H₂O), 1.533 Å (α-FeSO₃·3H₂O³⁹), 1.536 Å (β-FeSO₃·3H₂O⁴⁰) and 1.526 Å (MgSO₃·6H₂O³⁸).

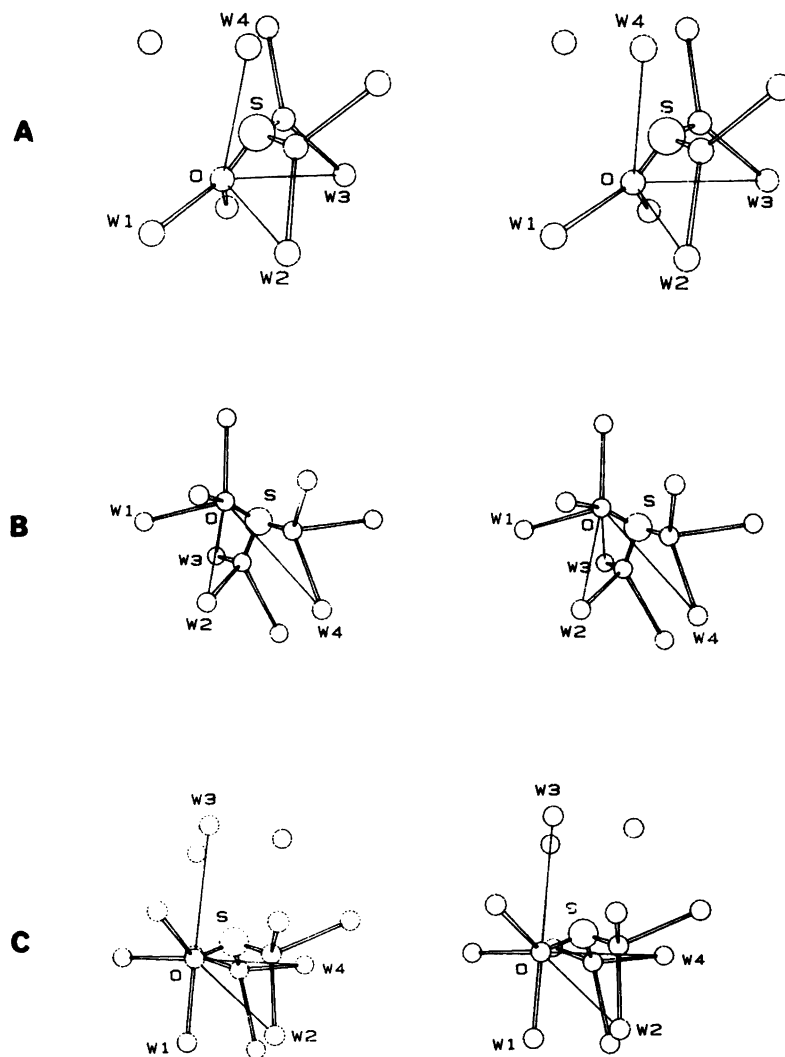


Fig. 5. Several hydration models of the sulfite ion (stereoview).

Fig. 6 B shows the experimental and theoretical radial distribution curves. Individual peak shapes (Fig. 6 A) have been calculated from the parameter values in Table 3 A. Fig. 7 represents the corresponding $s \cdot i(s)$ values.

As apparent from the residual curve in Fig. 6 B, there is no other significant peak less than 5 Å, though small ripples are still left, probably due to experimental uncertainties in the observed data. This indicates that the lone-pair of electrons of S(IV) is stereochemically active in solution in a similar way as found in the solid state.³⁶⁻⁴¹

3. Solution of ammonium disulfite (pH=5.1 and 5.3)

Before data analyses, the mol fractions of the hydrogen sulfite and the disulfite ions were estimated by the equilibrium constant given by Bourne *et al.*³ at an ionic strength of 2.0. The result indicated that the disulfite ion should be present predominantly, *i.e.* 80–90%, in the two measured solutions (*cf.* Table 1). In order to investigate if this distribution holds in our concentrated solutions, their Raman spectra were measured. The results were negative

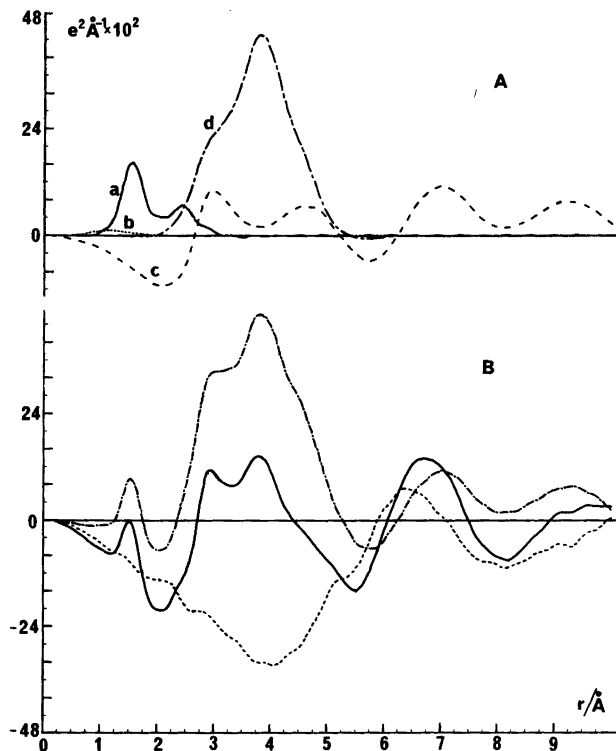


Fig. 6. (A) Peak shapes calculated for (a) the SO₃²⁻ ion, (b) the NH₄⁺ ion, (c) the bulk structure and (d) the hydration structure of the SO₃²⁻ ion (S–W, O–W(1), O–W(2), O–W(3) and O–W(4)). (B) Experimental (–) and theoretical (---) radial distribution curves with their difference (---) for the (NH₄)₂SO₃ solution.

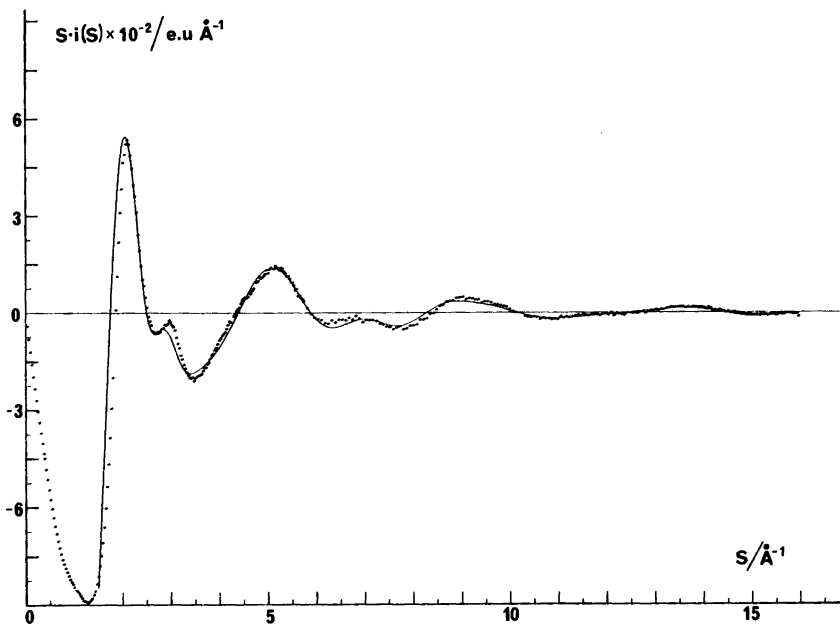


Fig. 7. Observed (dots) and calculated (solid line) $s \cdot i(s)$ values for the (NH₄)₂SO₃ solution.

for presence of the HSO_3^- ion (*cf.* Section 4). Therefore, the analysis of the diffraction data was made assuming presence of the disulfite ion only.

The radial distribution curves of the two ammonium disulfite solutions are shown in Figs. 1 C and D. The peak at 1.5 Å is due to the S–O interaction within the disulfite ion, in agreement with crystal structure determinations.^{43,44} The number of the S–O bonds of about five was preliminarily obtained from analysis of the peak area. This result prefers C_s symmetry for the structure of the $\text{S}_2\text{O}_5^{2-}$ ion, since C_{2v} symmetry structure containing an S–O–S bridge would require six S–O bonds. Another piece of evidence supporting the C_s symmetry structure is the peak centered at 2.35 Å which may correspond to four nearest neighbor O–O interactions within the $\text{S}_2\text{O}_5^{2-}$ ion. However, the position of the peak appears at a shorter distance than expected for the O–O interactions (2.42–2.47 Å^{43,44}) and the area under the peak could not be explained only by four O–O bonds (C_s symmetry) or six O–O bonds (C_s symmetry) within the $\text{S}_2\text{O}_5^{2-}$ ion. When the theoretical peaks calculated for five S–O and four nearest neighbor O–O bonds within the $\text{S}_2\text{O}_5^{2-}$ ion, parameter values of which were estimated from the distribution curves and the crystal structures,^{43,44} were subtracted from the original curve, a very significant difference peak appeared at around 2.20 Å (Fig. 9 C). The value agrees well with the S–S bond distance within the $\text{S}_2\text{O}_5^{2-}$ ion found in the crystal structures.^{44,45} The area under the peak is also in agreement with one S–S interaction. Thus, it is clearly evidenced that the $\text{S}_2\text{O}_5^{2-}$ ion has C_s symmetry containing an S–S bond in solution as has also been found in the crystal structures investigated so far.

The 3.8 Å peak may be attributed to the S–H₂O interaction as found in the sulfate and sulfite solutions.

The refinement of the structure of the S_2O_5 solution was performed in the following manner.

(a) The structure of the $\text{S}_2\text{O}_5^{2-}$ ion was described by two different S–O interactions, S–O(1) and S–O(2), an S–S bond, and nearest neighbor O–O interaction within each group (Fig. 8). The interactions between oxygen atoms within different groups were not included because of their small contribution to the reduced intensities.

(b) The interactions between the $\text{S}_2\text{O}_5^{2-}$ ion and nearest water molecules (or NH_4^+ ion) were taken into consideration by assuming n water molecules hydrogen bonded to disulfite oxygen atoms.

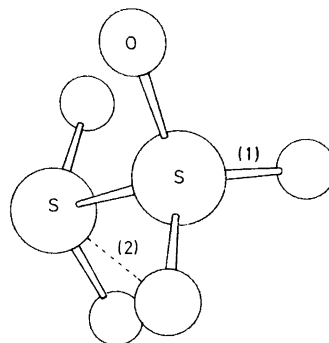


Fig. 8. The C_s symmetry structure of the disulfite ion.

The results of the refinements are given in Table 4. In refinement A, parameter $n_{\text{S-O}(1)}$ was allowed to vary in order to check the distribution of the HSO_3^- and the $\text{S}_2\text{O}_5^{2-}$ ions predicted from the thermodynamic data, and to confirm C_s symmetry structure of the $\text{S}_2\text{O}_5^{2-}$ ion. The relatively large temperature factor $b_{\text{S-S}}$ may indicate the existence

Table 4. The results of the least-squares refinements for A and B (see text) for the $(\text{NH}_4)_2\text{S}_2\text{O}_5$ solution (pH = 5.1) obtained in the range $3.0 < s < 15.0 \text{ \AA}^{-1}$. Standard deviations are given in parentheses.

		A	B
S–O(1)	r	1.498(2)	1.498(2)
	b	0.0025(2)	0.0030(2)
	n	4.80(4)	5
O–O	r	2.45(2)	2.42(2)
	b	0.003(1)	0.0011(9)
	n	4	4
S–S	r	2.236(11)	2.221(11)
	b	0.0051(7)	0.0052(7)
	n	1	1
S–O(2)	r	2.960 ^a	2.947 ^a
	b	0.015(1)	0.016(1)
	n	5	5
S–W (per $\text{S}_2\text{O}_5^{2-}$)	r	3.76(2)	3.77(2)
	b	0.031(1)	0.030(1)
	n	9.2(2)	8.9(2)
O–W (per $\text{S}_2\text{O}_5^{2-}$)	r	2.98(2)	2.98(2)
	b	0.017(2)	0.018(2)
	n	9.2 ^b	8.9 ^b
R-factor		0.101	0.104

^a Fixed to the value estimated from the geometry.

^b Assumed that $n_{\text{S-W}} = n_{\text{O-W}}$.

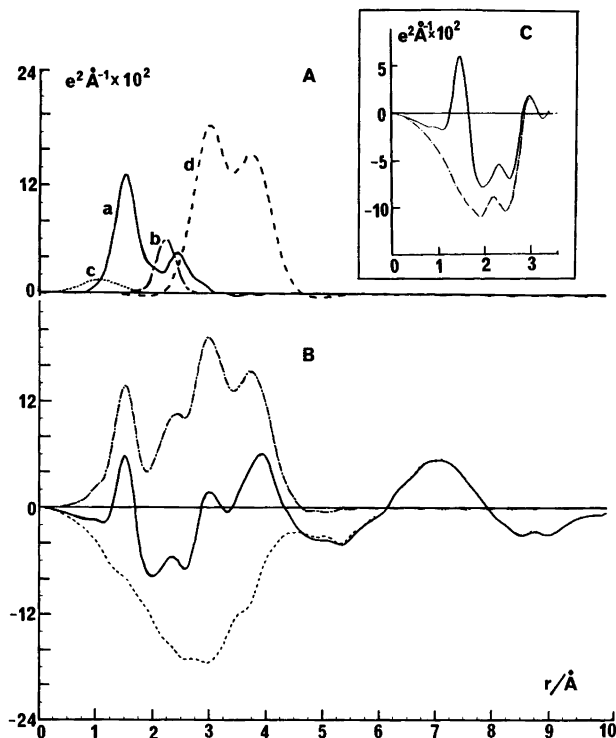


Fig. 9. (A) Peak shapes calculated for (a) S–O(1) and O–O bonds (b) the S–S bond and (c) N–H and O–H bonds within NH₄⁺ and H₂O, respectively. (B) Experimental (–) and theoretical (---) radial distribution curves and their difference (---) of the (NH₄)₂S₂O₅ solution (pH = 5.1). (C) The residual distribution curve (chain line) obtained by subtracting 5 × S–O(1) and 4 × O–O interactions within the S₂O₅²⁻ ion from the experimental distribution curve (solid line).

of a small fraction of HSO₃⁻ which is in accordance with the result from the equilibrium constant. The temperature factor of the S–O(1) bond is larger than those obtained for the S–O bonds in the sulfate and sulfite solutions (*cf.* Tables 2 and 3). This indicates the overlap of peaks due to different S–O bonds within the thionite and thionate groups. Attempts to refine their distances failed, however. The average S–O distance of 1.498(2) Å is in reasonable agreement with the weighted average S–O distance in the two groups found in the solid state (thionite: 1.431–1.472 Å, thionate: 1.495 and 1.499 Å).^{43,44}

The S–S bond distance has been found to be 2.221(11) Å, consistent with the crystal data (2.209 Å⁴³ and 2.170 Å⁴⁴).

The difference between experimental and theoretical radial distribution curves is shown in Fig. 9,

and the observed and calculated $s \cdot i(s)$ values in Fig. 10.

The value of n_{s-w} of about nine (*cf.* Table 4) implies that some water molecules or NH₄⁺ ions are shared between neighboring S₂O₅²⁻ ions since the content of water molecules and NH₄⁺ is not sufficient for hydration of the S₂O₅²⁻ ion. It is not possible to suggest any detailed hydration model of the disulfite ion in solution. However, the refinement results indicate that approximately nine water molecules are attached to the S₂O₅²⁻ ion with an S–H₂O distance of ~3.8 Å.

4. Raman spectra of the solutions

The Raman spectrum of the (NH₄)₂SO₄ solution showed four bands at 451(ν_2), 620(ν_4), 983(ν_1) and 1108(ν_3) cm⁻¹, characteristic for a tetrahedral

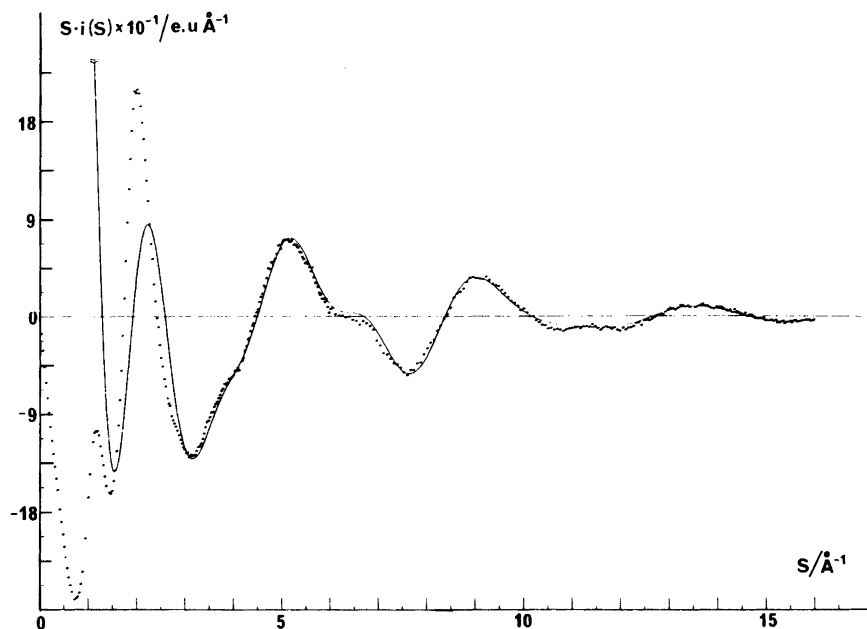


Fig. 10. Observed (dots) and calculated (solid line) $s \cdot i(s)$ values of the $(\text{NH}_4)_2\text{S}_2\text{O}_5$ solution (pH = 5.1).

SO_4^{2-} ion, while in the $(\text{NH}_4)_2\text{SO}_3$ solution three Raman bands appeared at 470(ν_4), 615(ν_2) and 960(ν_1 and ν_3), belonging to the sulfite ion.⁴ No other bands due to different species were observed.

Raman spectra of the $(\text{NH}_4)_2\text{S}_2\text{O}_5$ solutions were carefully measured in order to examine the formation of the hydrogen sulfite ion. In the two disulfite solutions, Raman bands appeared at 230, 430, 655 and 1050 cm^{-1} , all of which belong to the $\text{S}_2\text{O}_5^{2-}$ ion.⁶ Bands characteristic for the HSO_3^- ion should appear at 467, 1021, 1128 and 2533 cm^{-1} ,⁶ none of which could be observed for our solutions. It seems therefore reasonable to assume that the HSO_3^- ion is present only to a small extent in the concentrated solutions, probably less than suggested by the equilibrium study.³ Previous Raman spectra, measured for less concentrated solutions (1–2 M), have given bands corresponding to the HSO_3^- ion.⁶

Acknowledgements. The authors thank Professor Georg Lundgren for his kind interest in this study and Professor Kåre Larsson for making the Raman spectrophotometer available. The Swedish Natural Science Research Council is gratefully acknowledged for financial aid.

REFERENCES

1. Johansson, L.-G. and Vannerberg, N.-G. *Corros. Sci.* (1981). *In press.*
2. Brosset, C. *Kem. Tidskr.* 11 (1975) 92.
3. Bourne, D. W. A., Higuchi, T. and Pitman, I. H. *J. Pharm. Sci.* 63 (1974) 865.
4. Davis, A. R. and Chatterjee, R. M. *J. Solution Chem.* 4 (1975) 399.
5. Simon, A. and Schmidt, W. *Z. Electrochem.* 64 (1960) 737.
6. Meyer, B., Peter, L. and Shaskey-Rosenlund, C. *Spectrochim. Acta A* 35 (1979) 345.
7. Johansson, L.-G., Lindqvist, O. and Vannerberg, N.-G. *Acta Crystallogr. B* 36 (1980) 2523.
8. Simon, A., Waldmann, K. and Steger, E. *Z. Anorg. Allg. Chem.* 288 (1956) 131.
9. Herlinger, A. W. and Long, T. V. *Inorg. Chem.* 8 (1969) 2661.
10. Lindqvist, I. and Mörtzell, M. *Acta Crystallogr.* 10 (1957) 406.
11. Baggio, S. *Acta Crystallogr. B* 27 (1971) 517.
12. Linke, W. F. and Seidell, A., Eds., *Solubilities of Inorganic and Metal Organic Compounds*, 4th Ed., Am. Chem. Soc. 1965, Vol. 2, pp. 747–755.
13. Caminiti, R., Paschina, G., Pinna, G. and Magini, M. *Chem. Phys. Lett.* 64 (1979) 391.
14. Kolthoff, I. M., Sandell, E. B., Meehan, E. J. and Bruckenstein, S. *Quantitative Chemical Analysis*, 4th Ed., Macmillan, London 1971.

15. Johansson, G. *Acta Chem. Scand.* 20 (1966) 553.
16. Ohtaki, H., Maeda, M. and Ito, S. *Bull. Chem. Soc. Jpn.* 47 (1974) 2217.
17. Milberg, M. E. *J. Appl. Phys.* 29 (1958) 64.
18. Warren, B. E. and Mozzi, R. L. *Acta Crystallogr.* 21 (1966) 459.
19. Levy, H. A., Danford, M. D. and Narten, A. H. *Data Collection and Evaluation with an X-Ray Diffractometer Designed for the Study of Liquid Structure*, Report ORNL-3960, Oak Ridge National Laboratory, Oak Ridge 1966.
20. Sandström, M., Persson, I. and Ahrland, S. *Acta Chem. Scand. A* 32 (1978) 607.
21. Krogh-Moe, J. *Acta Crystallogr.* 9 (1956) 951.
22. Norman, N. *Acta Crystallogr.* 10 (1957) 951.
23. *International Tables for X-Ray Crystallography*, Kynoch Press, Birmingham 1974, Vol. 4.
24. Hajdu, F. *Acta Crystallogr. A* 28 (1972) 250.
25. Cromer, D. T. and Mann, J. B. *J. Chem. Phys.* 47 (1967) 1892.
26. Cromer, D. T. *J. Chem. Phys.* 50 (1969) 4857.
27. Compton, A. H. and Allison, S. K. *X-Rays in Theory and Experiment*, Van Nostrand-Reinhold, New York 1935.
28. Breit, G. *Phys. Rev.* 27 (1926) 362.
29. Dirac, P. A. M. *Proc. R. Soc. London A* 111 (1926) 405.
30. Johansson, G. and Sandström, M. *Chem. Scr.* 4 (1973) 195.
31. Ohtaki, H., Yamaguchi, T. and Maeda, M. *Bull. Chem. Soc. Jpn.* 49 (1976) 701.
32. Narten, A. H. *X-Ray Diffraction Data on Liquid Water in the Temperature Range 4°C–200°C*, Report ORNL-4578, Oak Ridge National Laboratory, Oak Ridge 1970.
33. Sillén, L. G. and Martell, A. E. *Stability Constants of Metal Ion Complexes, Special Publ. No. 25*, 1971.
34. Kjällman, T. and Olovsson, I. *Acta Crystallogr. B* 28 (1972) 1692.
35. Schlemper, E. O. and Hamilton, W. C. *J. Chem. Phys.* 44 (1966) 4498.
36. Battelle, L. F. and Trueblood, K. N. *Acta Crystallogr.* 19 (1965) 531.
37. Durand, P. J., Galigne, J. L. and Cot, L. *Acta Crystallogr. B* 33 (1977) 1414.
38. Flack, P. H. *Acta Crystallogr. B* 29 (1973) 656.
39. Johansson, L.-G. and Lindqvist, O. *Acta Crystallogr. B* 35 (1979) 1017.
40. Johansson, L.-G. and Ljungström, E. *Acta Crystallogr. B* 35 (1979) 2683.
41. Baggio, S. and Becka, L. N. *Acta Crystallogr. B* 25 (1969) 1150.
42. Kierkegaard, P., Larsson, L. O. and Nyberg, B. *Acta Chem. Scand.* 26 (1972) 218.
43. Lindqvist, I. and Mörtzell, M. *Acta Crystallogr.* 10 (1957) 406.
44. Baggio, S. *Acta Crystallogr. B* 27 (1971) 517.

Received September 18, 1981.